Differential topology and geometry of smooth embedded surfaces: selected topics

Frédéric Cazals, Marc Pouget

Differential topology and geometry of smooth embedded surfaces: selected topics

F. Cazals, M. Pouget

March 18, 2005

Abstract

The understanding of surfaces embedded in E^3 requires local and global concepts, which are respectively evocative of differential geometry and differential topology. While the local theory has been classical for decades, global objects such as the foliations defined by the lines of curvature, or the medial axis still pose challenging mathematical problems. This duality is also tangible from a practical perspective, since algorithms manipulating sampled smooth surfaces (meshes or point clouds) are more developed in the local than the global category. As a prerequisite for those interested in the development of algorithms for the manipulation of surfaces, we propose a concise overview of core concepts from differential topology applied to smooth embedded surfaces.

We first recall the classification of umbilics, of curvature lines, and describe the corresponding stable foliations. Next, fundamentals of contact and singularity theory are recalled, together with the classification of points induced by the contact of the surface with a sphere. This classification is further used to define ridges and their properties, and to recall the stratification properties of the medial axis. Finally, properties of the medial axis are used to present sufficient conditions ensuring that two embedded surfaces are ambient isotopic.

From a theoretical perspective, we expect this survey to ease the access to intricate notions scattered over several sources. From a practical standpoint, we hope it will be useful for those interested in certified approximations of smooth surfaces.

1 Introduction

1.1 Global differential patterns

Sampled surfaces represented either by point clouds or meshes are ubiquitous in computer graphics, computer aided design, medical imaging, computational geometry, finite element methods or geology. Aside from the situations where a sample surface is of self-interest —e.g. in computer graphics, sampled surfaces approximating (piecewise-)smooth surfaces are essentially found in two contexts which are surface reconstruction and surface discretization. In the first category, one is given a set of sample points acquired from a scanner (medical or laser) and wishes to reconstruct (by interpolation or approximation) the continuous or (piecewise-)smooth surface which has been sampled. In the second one, a surface is given implicitly or parametrically, and one wishes to discretize it for visualization or calculation purposes. In any case, three types of properties are usually of interest when comparing a (piecewise-)smooth surface and its discretization: topological and geometric properties, local differential properties, and global differential properties.

From a topological standpoint, one expects the surfaces to be homeomorphic or even better isotopic. Example algorithms with such a guarantee are [1, 2] in the surface reconstruction area, and [3, 4] in the surface meshing context. Apart from these algorithms, the interested reader should consult [5, 6] where sufficient conditions on isotopy can be found. It should also be pointed out that the hypothesis under which one achieves these properties usually also yield a bound on the Hausdorff distance between the surfaces, a property of geometric nature.

Local differential properties are of two types, namely intrinsic and extrinsic. For extrinsic quantities, one wishes to guarantee that the tangent plane (at the first order), the principal directions and curvatures (at the second order), or higher order coefficients (e.g. curvature extremality coefficients) are close.

The development of algorithms providing such guarantees has been subject to intense research [7], and recent advances provide guarantees either point-wise [8, 9] or in the geometric measure theory sense [10]. Although extrinsic properties are usually the properties sought, some applications care for intrinsic faithfulness. These applications are usually concerned with the question of flattening / parameterizing a surface, and the reader is referred to [11] for an example related to geology, together with the ensuing conditions.

At last, global differential properties usually refer to guarantees on loci of points having a prescribed differential property. Example such loci are lines of curvature, ridges, or the medial axis. Applications involving such patterns are surface remeshing [12], scientific visualization [13], feature extraction [14, 15, 16], or surface reconstruction [17, 18] and related topics [19]. Providing such guarantees faces the difficulties afore-mentioned. Not only point-wise estimates must be reliable, but they must also be connected correctly at the surface level. This difficulties are tangible from a practical perspective, and to the best of our knowledge, even under reasonable assumptions, no algorithm as of today is able to report any global differential pattern with some guarantee — a topologically correct medial axis or foliation from a sampled surface.

The lack of such algorithms is partly due to the fact that global differential patterns have an involved structure described in differential topology and singularity theory sources. Easing the access to these notions is the incentive of this concise survey, which deliberately focuses on selected topics related to the geometry and topology on embedded surfaces. In selecting these topics, we had to make choices and omitted the following themes: symmetry sets [20]; distance functions used in analysis [21], optimization [22], mathematical morphology [23], and geometric modeling [24]; bifurcations of symmetry sets and medial axis [25, 26]; differential geometry of skeletal structures [27]; practical algorithms to extract medial axis [28] or ridges and related objects [29].

Our presentation focuses on the geometric intuition rather than the technicalities. From a practical standpoint, we hope it will be helpful for those aiming at producing globally coherent approximations of surfaces.

1.2 Paper overview

Following a natural trend, we successively examine differential topology concepts of the second order (umbilics, lines of curvatures, foliations) and the third order (ridges, medial axis). To finish up, selected properties of the medial axis are used to specify the topological equivalence between embedded surfaces.

More precisely, the Monge form of a surface is recalled in section 2. Second order properties are presented in section 3 —umbilics and lines of curvature. The classification of contact points between the surface and spheres is presented in section 4. This classification is used in section 5 to recall the stratification properties of the medial axis. Finally, the topological equivalence between embedded surfaces is recalled in section 6, and sufficient conditions involving the medial axis are also presented.

2 The Monge form of a surface

2.1 Generic surfaces

Our focus is on generic phenomena on surfaces, and the statements presented are valid for generic surfaces only. Formally if one considers the set of all smooth surfaces M in E^3 as an infinite dimensional space with a well defined topology, a property is generic if the surfaces exhibiting this property form an open dense subset. Informally this notion means that a generic property remains valid if one allows random perturbations. Due to the infinite dimension of the space of surfaces, it is not straightforward to define a topology on this set. We will consider the C^r topology ($r \in \mathbb{N} \cup \{\infty\}$) on the set of all smooth oriented surfaces M embedded in the Euclidean space E^3 (cf. [30, p.27]). A sequence M_n of surfaces converges to M in the C^r sense provided there is a sequence of real functions f_n on M such that $M_n = (I + f_n N)(S)$, where I is the identity of E^3, N is the normal vector of M and f_n tends to 0 in the C^r sense. That is, for every chart (u, v) with inverse parameterization X, $f_n \circ X$ converges to 0 together with the partial derivatives of order r, on compact parts of the domain of X.

2.2 The Monge form of a surface

We consider a surface S embedded in the Euclidean space E^3 equipped with the orientation of its world coordinate system —referred to as the *direct orientation* in the sequel. At any point of the surface which is not an umbilic, principal directions are well defined, and the (non oriented) principal directions d_1, d_2 together with the normal vector n define two direct orthonormal frames. If v_1 is a unit vector of direction d_1 then there exists a unique unit vector v_2 so that (v_1, v_2, n) is direct; and the other possible frame is $(-v_1, -v_2, n)$. In one of these, and as long as our study is a local differential one, the surface is assumed to be given as a Monge patch at the origin [16] —with *h.o.t* standing for *higher order terms*:

$$z = \frac{1}{2}(k_1x^2 + k_2y^2) + \frac{1}{6}(b_0x^3 + 3b_1x^2y + 3b_2xy^2 + b_3y^3) \tag{1}$$

$$+ \frac{1}{24}(c_0x^4 + 4c_1x^3y + 6c_2x^2y^2 + 4c_3xy^3 + c_4y^4) + h.o.t \tag{2}$$

Occasionally, we shall refer to the cubic part $C_M(x, y)$ as the Monge cubic, that is:

$$C_M(x, y) = b_0x^3 + b_1x^2y + b_2xy^2 + b_3y^3. \tag{3}$$

If the origin is not an umbilic, the principal direction d_1 (resp. d_2) associated to the principal curvature k_1 (resp. k_2) is the x (resp. y) axis. We shall always assume that $k_1 \geq k_2$ and we consider 'blue' (resp. 'red') something special happening with k_1 (resp. k_2). For example the blue focal surface is the set of centers of curvature associated to the blue curvature k_1. Note that a change of the normal surface orientation swaps the colors.

Away from umbilics, local analysis of the principal curvatures can be done for the Monge coordinate system and along the curvature lines. The Taylor expansion of the principal curvature k_1 in the Monge coordinate system is

$$k_1(x, y) = k_1 + b_0x + b_1y + (\frac{c_0 - 3k_1^2}{2} + \frac{b_1^2}{k_1 - k_2})x^2 \tag{4}$$

$$+ (c_1 + \frac{2b_1b_2}{k_1 - k_2})xy + (\frac{c_2 - k_1k_2^2}{2} + \frac{b_2^2}{k_1 - k_2})y^2 + h.o.t \tag{5}$$

The Taylor expansion of k_1 (resp. k_2) along the blue (resp. red) curvature line going through the origin and parameterized by x (resp. y) are:

$$k_1(x) = k_1 + b_0x + \frac{P_1}{2(k_1 - k_2)}x^2 + h.o.t \qquad P_1 = 3b_1^2 + (k_1 - k_2)(c_0 - 3k_1^3). \tag{6}$$

$$k_2(y) = k_2 + b_3y + \frac{P_2}{2(k_2 - k_1)}y^2 + h.o.t \qquad P_2 = 3b_2^2 + (k_2 - k_1)(c_4 - 3k_2^3). \tag{7}$$

Notice also that switching from one of the two coordinate systems mentioned in introduction to the other reverts the sign of all the odd coefficients on the Monge form of the surface.

Some notions about cubics will be useful in the sequel.

Definition. 1 *A real cubic $C(x, y)$ is a bivariate homogeneous polynomial of degree three, that is $C(x, y) = b_0x^3 + 3b_1x^2y + 3b_2xy^2 + b_3y^3$. Its discriminant is defined by $\delta(C) = 4(b_1^2 - b_0b_2)(b_2^2 - b_1b_3) - (b_0b_3 - b_1b_2)^2$.*

A cubic factorizes as a product of three polynomials of degree one with complex coefficients, called its factor lines. In the (x, y) plane, a real factor line defines a direction along which C vanishes. The number of real factor lines depends on the discriminant of the cubic and we have

Proposition. 1 *Let C be a real cubic and δ its discriminant. If $\delta > 0$ then there are 3 distinct real factors, if $\delta < 0$ there is only one real factor.*

In the particular description of surfaces as Monge patches, we have a family of Monge patches with two degrees of freedom —the dimension of the manifold. A property requiring 1 (resp. 2) condition(s) on this family is expected to appear on lines (resp. isolated points) of the surface —a condition being an equation involving the Monge coefficients. A property requiring at least three conditions is not generic. As an example, ridge points (characterized by the condition $b_0 = 0$ or $b_3 = 0$) appears on lines and umbilics (the two conditions are $k_1 = k_2$ and the coefficient of the xy term vanishes) are isolated points. A flat umbilic, requiring the additional condition $k_1 = 0$, is not generic.

3 Umbilics and lines of curvature, principal foliations

This section is devoted to second order properties on a surface, and more precisely to umbilics and lines of curvature. General references are [31, 32, 30, 16, 33].

3.1 Classification of umbilics

To present the classification of umbilics, let us first recall some facts about lines of curvature. On each point of the set S' defined as the surface S except its umbilics, the two principal directions are well defined and orthogonal. They define two direction fields on S', one everywhere orthogonal to the other, so it is sufficient to study only one of these. Each principal direction field defines lines of curvature. The set of all these lines, called the principal foliation, will be studied in the next section.

Definition. 2 *A line of curvature is an integral curve of the principal field, that is a regular curve on S' which is everywhere tangent to the principal direction and is maximal for inclusion (it contains any regular curve with this property which intersects it).*

The index of an umbilic describes the way the lines of curvature turn around the umbilic. The index of a direction field at a point is $(1/2\pi)\int_0^{2\pi}\theta(r)dr$, where $\theta(r)$ is the angle between the direction of the field and some fixed direction, and the integral is taken over a small counterclockwise circuit around the point. For generic umbilics this index is $\pm 1/2$, this implies that the direction field is not orientable on a neighborhood of such points. As illustrated on Fig. 1, if one fixes an orientation of the field at a point on a circuit around an umbilic, propagating this orientation by continuity along the circuit gives the reverse orientation after one turn. In other words, there is no non vanishing continuous vector field inducing the direction field around the umbilic. The index can also be computed with the Monge cubic, this computation is point wise as opposed to the previous one, but need third order coefficients (hence it is likely to be less stable in practice). Let $S = (b_0 - b_2)b_2 - b_1(b_1 - b_3)$,

- if $S < 0$ then the index is $-1/2$ and the umbilic is called a star,
- if $S > 0$ then the index is $+1/2$ and we have to do more calculations to distinguish between the so called lemon and monstar.

A finer classification is required to distinguish between the two umbilics of index $+1/2$. We shall need the following:

Definition. 3 *Consider an umbilic p and denote T_pS the tangent plane of the surface at p. A* limiting principal direction *is a direction of T_pS which is tangent to a line of curvature which end at the umbilic.*

Limiting principal directions are related to the Jacobian cubic of the umbilic (cf. [16]):

$$J_C = B_0x^3 + 3B_1x^2y + 3B_2xy^2 + B_3y^3 = b_1x^3 + (2b_2 - b_0)x^2y - (2b_1 - b_3)xy^2 - b_2y^3. \tag{8}$$

The real factor lines of this form are the limiting principal directions at the umbilic. As recalled by proposition 1, the number of such directions depends on the discriminant U of J_C:

- If $U < 0$ then there is one limiting principal direction, necessarily $S > 0$ and the umbilic is called a lemon.
- If $U > 0$ then there are three limiting principal directions, furthermore if $S < 0$ the umbilic is a star else $S > 0$ and it is called a monstar. For a monstar, the three directions are contained within a right angle and all the curvature lines in this angle end at the umbilic and form the parabolic sector of the monstar. Note that all these lines have the same tangent at the umbilic: the limiting principal direction inside the parabolic sector. For a star, only three lines of curvature end at the umbilic and the limiting directions are not contained in a right angle.

We summarize the previous discussion as follow:

Theorem. 1 *There are three classes of generic umbilics in the C^3 sense, namely Lemons, Monstar and Stars. They are distinguished by their index and the number of limiting principal directions.*

To be an umbilic requires two conditions on the Monge coefficients, this implies that the cases $S = 0$ or $U = 0$ are not generic umbilics. From the same argument, a generic umbilic is a non flat point: its Gaussian curvature does not vanish, and generic umbilics are isolated (cf. [32, p.184]).

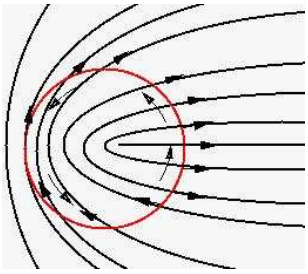

Figure 1: Impossibility of a global orientation around an umbilic

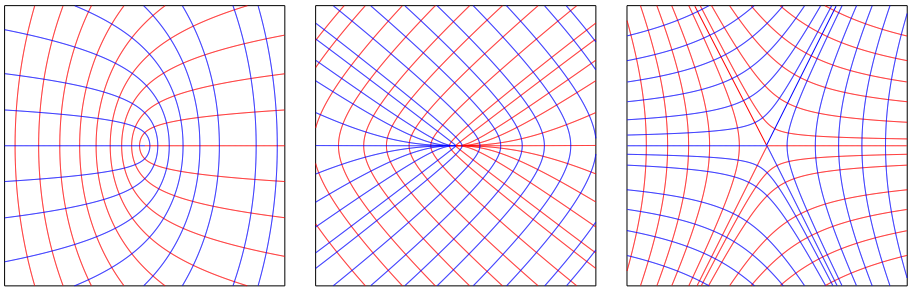

Figure 2: Umbilics: Lemon and Monstar of index +1/2, Star of index -1/2.

3.2 Principal foliations

Recall that the blue (resp. red) principal foliation is the set of all blue (resp. red) curvature lines defined on S'. The umbilics can be regarded as singular points for these foliations if one wishes to consider them on S. The first element required concerns the topology of a curvature line. A line of curvature γ is either homeomorphic to:

- an open interval $I = (\omega_-, \omega_+)$, then it is assumed to be oriented and parameterized by this interval. Its $\alpha(\gamma)$ (resp. $\omega(\gamma)$) limit set is the collection of limit points of sequences $\gamma(s_n)$, convergent in S, with s_n tending to ω_- (resp. ω_+). The limit set of γ is the union $\alpha(\gamma) \cup \omega(\gamma)$.
- or to a circle, then it is called a cycle. It is hyperbolic if its Poincaré return map π is so that $\pi' \neq 1$. In other words, if one orients an hyperbolic cycle, the lines of curvature can be oriented on a neighborhood of this cycle by continuity and they are all attracted or repelled on both sides of the cycle (cf. Fig. 3).

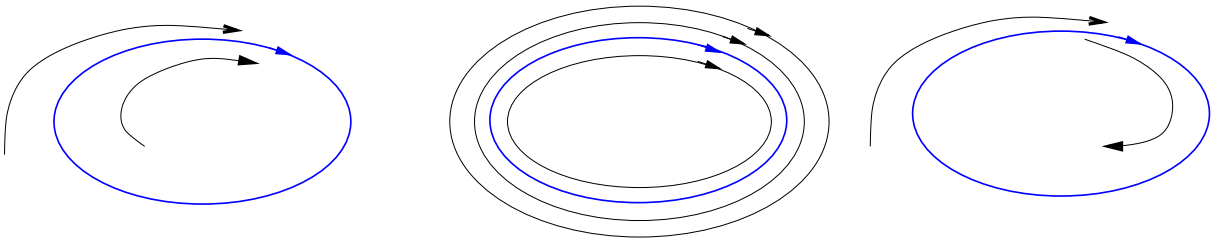

Figure 3: A hyperbolic cycle and two non hyperbolic ones

Special lines divide the set of all curvature lines in the vicinity of an umbilic into sectors, they are separatrices.

Definition. 4 *A separatrix is a line of curvature with an umbilic in its limit set and so that there exists arbitrarily close to that line, another line without this umbilic in its limit set.*

A sector defined by two consecutive separatrices is

- hyperbolic if none of the lines in the sector have the umbilic in their limit set;
- parabolic if all curvature lines in the sector have the umbilic in their α or exclusive ω limit set;

The alternative case of an elliptic sector, if all curvature lines in the sector have the umbilic in their α and ω limit set, is not generic —cf. Nikolaev [34, p.360]. Note that a separatrix is a line of curvature which ends at an umbilic, hence its tangent at this point is a limiting principal direction. But the limiting principal direction inside the parabolic sector of a monstar is not tangent to a separatrix of this umbilic —because all lines in a neighborhood have the monstar in their limit set. This explains another classification of umbilics from Darboux based on the number of separatrices. This classification rephrases the previous one: a lemon or D_1 has one separatrix, a monstar or D_2 has two and a star or D_3 has three.

The next result [30, p.27] describes stable configuration of the principal foliations for smooth compact oriented surfaces embedded in E^3. A surface M is said to be C^r principal structurally stable if for every sequence S_n converging to S in the C^r sense, there is a sequence of homeomorphisms H_n from M_n onto M, which converges to the identity of M, such that, for n big enough, H_n is a principal equivalence from M_n onto M. That is H_n maps the umbilical set of M_n onto the umbilical set of M, and maps the lines of the principal foliations of M_n onto those of M.

Theorem. 2 *Let Σ be the subset of smooth compact oriented surfaces which satisfies the following four conditions:*

- *all the umbilic points are of type D_i, $i = 1, \ldots, 3$;*
- *all the cycles are hyperbolic;*
- *the limit sets of every line of curvature are umbilics or cycles;*
- *all the separatrices are separatrices of a single umbilic (they cannot connect two umbilics or twice the same one being separatrices at both ends).*

Then Σ is open and each of its elements is principal structurally stable in the C^3-sense, Σ is dense in the C^2-sense.

This theorem implies that stable principal foliations are described with the set of umbilics, cycles and the way the separatrices connect these elements. The complement of these features on the surface S then decomposes on canonical regions of two types parallel and cylindrical. On each region, the limit sets of all lines are the same: a cycle or a D_2 umbilical point (through its parabolic sector). A region is parallel if there are separatrices in its boundary. If the boundary consists only of cycles then the region is cylindrical.

The topology of the surface S constrains the number and the type of umbilics. More precisely, the sum of indices of umbilics must be the Euler characteristic $\chi(S)$ —[35, p.223]. Moreover, the principal foliation defines a bipartite graph $G(V_1, V_2, E)$ with V_1 the set of umbilics, V_2 the set of cycles and parabolic sectors and E the set of separatrices. The edges connect elements of V_1 to elements of V_2 with the following constraints.

- A D_i umbilic has i incident edges.
- Since there is no elliptic sector, a separatrix of a D_2 umbilic cannot be connected to its parabolic sector.
- The graph is embedded on the surface without intersecting the separatrices.

4 Contacts of the surface with spheres, Ridges

To classify points of a smooth surface regarding curvature properties, we first recall fundamentals from contact and singularity theory. Following [36, 37, 31], we probe a point of the surface with a sphere centered along the normal at that point. Working out the dominant terms of the Taylor expansion of the probe function yields the classification of points desired. General references for this section are [38], [32] or [39].

4.1 Distance function and contact function

A standard way to classify points on a smooth surface consists of using contact theory. Consider a portion of surface locally parameterized in a chart $(U, p(x, y))$ with $U \subset \mathbb{R}^2$, $(x_0, y_0) \in U$ and a sphere C of center c. Denoting $<,>$, the standard inner product of E^3, the contact function at the point $p(x_0, y_0) \in S$ is the function defined by:

$$g : U \times \mathbb{R}^3 \mapsto \mathbb{R},\ g((x, y), c) =< p(x, y)c, p(x, y)c > - < p(x_0, y_0)c, p(x_0, y_0)c > . \tag{9}$$

This function is just the square distance from the surface to the center of the sphere minus the square of its radius $r^2 =< p(x_0, y_0)c, p(x_0, y_0)c >$. The intersection points between S and C have coordinates $(x, y, p(x, y))$ satisfying $g(x, y) = 0$. The philosophy of contact theory is the following. Once the center of the sphere have been chosen, the contact function is a bivariate function. Then, we wish to report the possible *normal forms* of g as a bivariate function.

Before illustrating this process, let us observe that if the center of the sphere C is not contained in the affine space defined by the contact point and the normal at the surface S there, then the intersection between S and C is transverse, which does not reveal much about S at p. Studying the nature of the contact really starts with a center aligned with the normal, and we shall see that the cases encountered actually yield a decomposition of the normal bundle [1] of the surface.

Rmk. Note that if one of the principal curvature vanishes, one can assume the center of the principal sphere is at infinity. This means that the relevant contact to be considered is that of a plane with the surface at such a point. One can find a precise description of these parabolic points in [16].

4.2 Generic contacts between a sphere and a surface

Before presenting the generic contacts, let us illustrate the process of finding the first normal form using the Morse lemma. To ease the calculations, assume that the contact point is the origin, that the surface is given in Monge form, and that the center of the sphere has coordinates $c(0, 0, r)$. Then, the contact function simplifies to:

$$g(x, y) = x^2 + y^2 + (z - r)^2 - r^2 =< pc, pc > -r^2. \tag{10}$$

Using the Monge form of f, one gets the following expansion:

$$g(x, y) = x^2(1 - rk_1) + y^2(1 - rk_2) - \frac{r}{3}C_M(x, y) + h.o.t \tag{11}$$

The expansion does not contain linear terms and the origin is therefore a critical point. Moreover, if $r \neq 1/k_1$ and $r \neq 1/k_2$, the critical point is non-degenerate. By the Morse lemma, the contact function rewrites as $g = \pm x^2 \pm y^2$ up to a diffeomorphism. If the coefficients of both variables have the same sign, then the intersection between S and C reduces to point. Otherwise, the intersection consists of two curves.

The previous discussion is typical from singularity theory. Assuming $r \neq 1/k_1$ and $r \neq k_2$, we worked out the the *normal* form of a multivariate function, thus highlighting its dominant terms. In the sequel, we shall just state and use the classification of generic singularities of the contact function. As illustrated by Morse's lemma, it is important to observe that the normal form is exact, i.e. does not hide any higher order term. We shall need the following:

[1] The normal bundle of the surface is the three-dimensional manifold obtained by adding to each point of the surface a one-dimensional affine space defined by the pair (point, normal).

Definition. 5 *Let $f(x, y)$ be a smooth bivariate function. Function f has an A_k or D_k singularity if, up to a diffeomorphism, it can be written as:*

$$\begin{cases} A_k : f = \pm x^2 \pm y^{k+1}, \ k \geq 0, \\ D_k : f = \pm yx^2 \pm y^{k-1}, \ k \geq 4. \end{cases} \tag{12}$$

The singularity is further denoted $A_k^{\pm}$ or $D_k^{\pm}$ if the product of the coefficients of the monomials is ± 1.

As subsumed by this definition, an A_k singularity precludes an A_{k+1} singularity, and similarly for D_k. An important characteristic of these normal forms is their zero level set. Those of the A_k sequence are illustrated on Fig. 4, where the (branches of) curves are defined from $x = \pm y^{(k+1)/2}$. More precisely:

Observation. 1 *The zero level set of an A_0 singularity consists of a smooth curve, and that of an A_{2p} singularity for $p \geq 1$ of one curve having a cusp at the origin. The zero level set of an A_{2p-1} singularity consists of two tangential curves or an isolated point depending on the product of the signs of the monomials.*

For a D_k singularity, since $f = y(\pm x^2 \pm y^{k-2})$, the line $y = 0$ is always solution. For the other solutions, the discussion is identical to the A_k case.

Observation. 2 *The zero level set of an D_{2p}^+ (D_{2p}^-) singularity consists of one (three) curve(s). The zero level set of an D_{2p+1}^+ or D_{2p+1}^- singularity consists of two curves.*

The classification of generic contact points is the following [36, 37]:

Theorem. 3 *The generic singularities of the contact function between a sphere and a surface are of type A_0, A_1, A_2, A_3, A_4, D_4.*

The A_0 contact is just the transverse intersection mentioned at the beginning of this section, and we shall not discuss it further. The others types of contacts —respectively A_k and D_k— encode properties of the surface away from umbilics and at umbilics.

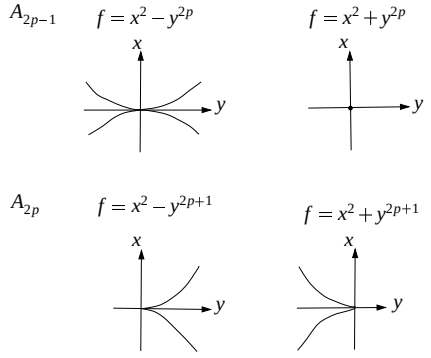

Figure 4: Zero level sets of the $A_k : f = x^2 \pm y^{k+1}$ singularities

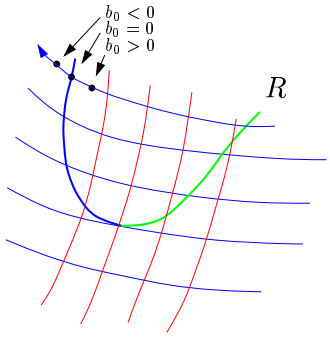

Figure 5: Variation of the b_0 coefficient and turning point of a ridge

4.3 Contact points away from umbilics

We proceed with the discussion of the contacts away from umbilics.

A_1 **contact.** $[r = 1/k_1, r \neq 1/k_2]$ The origin is a non degenerate critical point. The intersection reduces to one point or consists of two curves depending on the value of r wrt $1/k_2$ and $1/k_2$.

A_2 **contact.** $[r = 1/k_1, b_0 \neq 0$ (or $r = 1/k_2, b_3 \neq 0)]$ The sphere is a sphere of principal curvature, and the curvature is not an extremum by Eq. (6) since $b_0 \neq 0$. Due to the presence of terms of odd degree in the normal form, the intersection between the sphere and the surface is not reduced to a point (cf. Fig. 6 and 7).

A_3 **contact.** $[r = 1/k_1, b_0 = 0, P_1 \neq 0$ (or $r = 1/k_2, b_3 = 0$, $P_2 \neq 0)]$ The sphere is a sphere of principal curvature, and the principal curvature has a local extremum since $b_0 = 0$ and $P_1 \neq 0$ —or $b_0 = 3$ and $P_2 \neq 0$. An A_3 contact defines a *ridge* point, but not all ridge points are A_3 points —see the turning points below. Distinguishing further between A_3^- and A_3^+ yields the distinction between elliptic and hyperbolic ridge points [2]:

- Elliptic. If $P_1 < 0$, the contact function has A_3^+ singularity and its normal form is $g = y^2 + x^4$. Equivalently, the blue curvature is maximal along its curvature line. The blue sphere of curvature has a local intersection with M reduced to p (cf. Fig. 8).
- Hyperbolic. If $P_1 > 0$, the contact function has an A_3^- singularity and its normal form is $g = y^2 - x^4$. Equivalently, the blue curvature is minimal along its line. The local intersection of the blue sphere of curvature with M is two tangential curves (cf. Fig. 9).

Summarizing, $b_0 = 0, P_1 \neq 0$ defines a blue ridge point, either elliptic or hyperbolic. Similarly, $b_3 = 0$ defines a red ridge point, whose type is specified by the sign of P_2 defined by Eq. (7). A red ridge is elliptic if k_2 is minimal ($P_2 < 0$) along its curve and hyperbolic if k_2 is maximal ($P_2 > 0$). (Notice that in Eq. (7) the sign of P_2 is in accordance with the negative sign of $k_2 - k_1$.)

Notice that the type, elliptic or hyperbolic, is independent of the surface orientation. Ridge points are on smooth curves on the surface called ridge lines and can be colored according to the color of the points. Away from umbilics, a blue ridge can cross a red ridge at a ridge point colored blue and red that we call a purple point. A crossing of ridges of the same color is not generic.

Remark. When displaying ridges, we shall adopt the following conventions:

- blue elliptic (hyperbolic) ridges are painted in blue (green),
- red elliptic (hyperbolic) ridges are painted in red (yellow).

A_4 **contact.** $[r = 1/k_1, b_0 = 0, P_1 = 0$ (or $r = 1/k_2, b_3 = 0$, $P_2 = 0)]$ The blue curvature has a infection along its line ($k_1' = k_1'' = 0$ but $k_1''' \neq 0$, derivatives shall be understood as along the curvature line, cf Eq. (6). As an A_4 singularity, the local intersection of the blue sphere of curvature with M is a curve with a cusp at the contact point. Such a point is called a *ridge turning point*. At such a point, the ridge is tangent to the line of curvature of the same color, and the ridge changes from elliptic to hyperbolic —from a maximum to a minimum of the principal curvature.

The variation of the b_0 coefficient in the neighborhood of a blue ridge and a turning point of such a ridge are illustrated on Fig. 5. Summarizing the previous observations, we have:

Definition. 6 *Let $p \in M$ be a non-umbilical point, then p is a blue ridge point if one of the following equivalent conditions is satisfied:*

(i) the blue principal curvature has an extremum along the corresponding blue line of curvature,

(ii) $b_0 = 0$,

(iii) the blue sphere of curvature has at least an A_3 contact with M at p.

Notice again that a contact involves a sphere and the surface. The contact therefore provides information on the surface but also on its focal surfaces —the blue/red one assuming the the sphere in contact is a principal blue/red sphere of curvature. The reader is referred to [20] for local models of the focal at such singularities. We actually have the following:

Observation. 3 *At a ridge point, the focal surface is not regular —the center of the osculating sphere is located on a cuspidal edge of the focal surface.*

[2] Elliptic and hyperbolic ridge points are called sterile and fertile by Porteous. This refers to the possibility for umbilics to appear near such ridges.

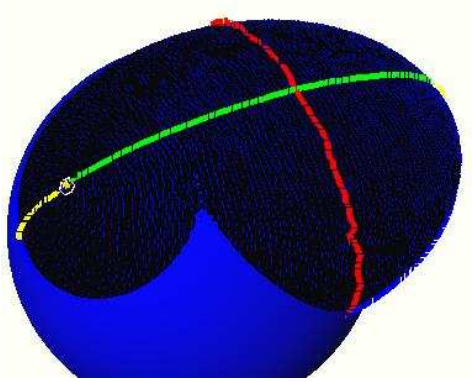

Figure 6: A_2 contact with the blue sphere

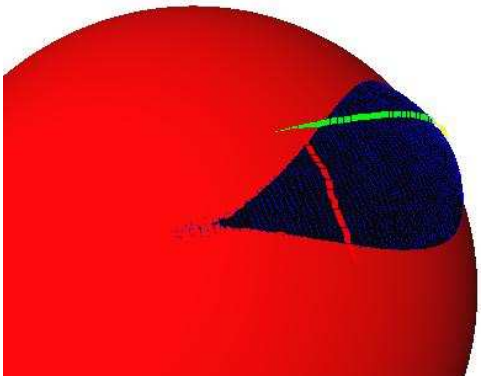

Figure 7: A_2 contact with the red sphere

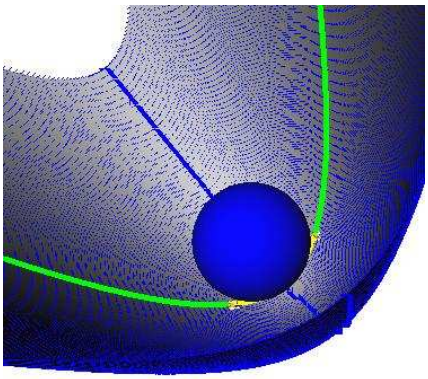

Figure 8: A_3^+ contact of the blue sphere of curvature at a blue elliptic ridge point (on the blue curve)

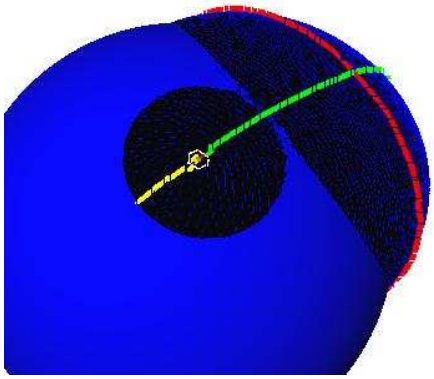

Figure 9: A_3^- contact of the blue sphere of curvature at a blue Hyperbolic ridge point (on the green curve)

4.4 Contact points at umbilics

Away from umbilic, the x and y coordinates of the Monge coordinate system follow the principal directions; at the umbilic there is no such canonical choice of coordinates, hence the values of $b_0 \neq 0$ and $b_3 \neq 0$ are not relevant and other invariants must be considered.

To see which ones, consider the contact function given by Eq. (11). Since $r = 1/k_1 = 1/k_2$, it is dominated by the cubic terms. More precisely, the singularity is generically a $D_4^{\pm}$. The number of ridges passing through the umbilic is the number of curves in the zero level set of contact function. Hence this number reads on the normal form, and is equal to one or three as mentioned in observation 2. This fact is not intuitive and it is neither obvious that ridges pass through umbilics. A way to explain these facts is to study the gradient field ∇k_1 (the same holds for ∇k_2) well defined at non umbilical points. Indeed a non-umbilical blue ridge point can be seen as a point on a blue curvature line where ∇k_1 is orthogonal to the curve that is $< \nabla k_1, d_1 >= 0$, or equivalently the iso-curve of k_1 is tangent to the curvature line. Hence one has to study orthogonality between the two fields ∇k_1 and d_1. In section 3.1, it has been shown that the index of the d_1 fields distinguishes stars (index -1/2) from lemons or monstars (index $+1/2$). The study of k_1 and ∇k_1 shows that generically, one has the following:

- k_1 has a minimum, then the vector field ∇k_1 has index 1; this also implies that the umbilic is a star and that there are 3 directions in which $< \nabla k_1, d_1 >= 0$;
- there is a curve along which $k_1 = k$ is constant passing through the umbilic, then ∇k_1 has index 0 and there is 1 direction in which $< \nabla k_1, d_1 >= 0$.

The distinction between these two cases also reads on the Monge cubic C_M, its number of real factor lines is the number of ridges, hence it depends on the sign of its discriminant $D = \delta(C_M)$. One can summarize the previous discussion as follow —see also Fig. 17:

Theorem. 4 *Generic umbilics are of two types:*

- *Elliptic or 3-ridge umbilic. The Monge cubic has three different real factor lines, or equivalently the contact function has a D_4^- singularity, and three ridge lines cross at the umbilic. Moreover at the umbilic, k_1 has a minimum and k_2 a maximum. Such an umbilic is a star.*
- *Hyperbolic or 1-ridge umbilic. The Monge cubic has only one real factor line, or equivalently the contact function has a D_4^+ singularity, and one ridge passes through the umbilic. Moreover passing through the umbilic, there is one curve along which k_1 (resp. k_2) is constant equal to k. Such an umbilic is either a lemon, a monstar or a star.*

The number of ridges is given by the number of real factors lines of the Monge cubic, but these lines are not the tangent directions to ridge lines going through the umbilic. However, these tangent directions can be computed from the Monge cubic cf. [16].

The intersection between the surface and its osculating sphere at an umbilic is not reduced to a point (cf. Observation 2). This fact remains true close to the umbilic and in particular on ridges, so we have:

Observation. 4 *A ridge passing through an umbilic must be hyperbolic.*

It also turns out that ridges are smooth curves crossing transversally at the umbilic and changing color there —from a minimum of k_1 to a maximum of k_2. Notice that a ridge may not pass through an umbilic, then it is of a single color and changes type at each turning point if any —there is an even number of such points.

Rmk. A finer distinction of elliptic umbilics concerns the ordering of ridge colors around the umbilic: it is called symmetrical if ridges alternate colors RBRBRB (then $T = b_0^2 + b_3^2 + 3(b_0 b_2 + b_1 b_3) < 0$) and unsymmetrical if the ordering is RRRBBB ($T > 0$). Figure 10 gives a schematic view of ridges at umbilics, more accurate figures can be found in [16].

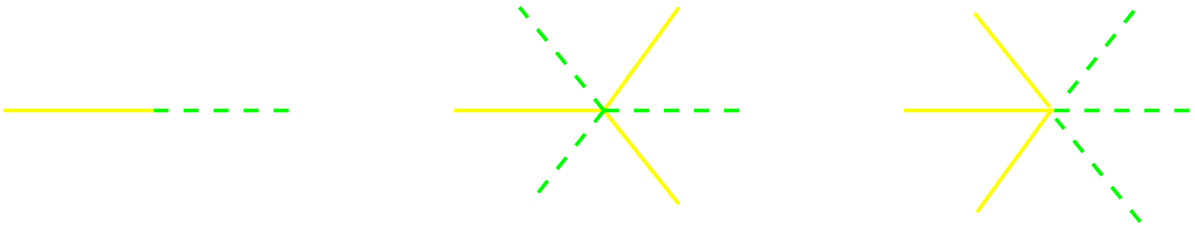

Hyperbolic umbilic | Symmetric elliptic umbilic | unsymmetric elliptic umbilic

Figure 10: Ridges at umbilic

4.5 Illustrations

We illustrate the previous global structure theorems on the famous example of an ellipsoid with three different axes —Fig. 11, an implicit blend of two ellipsoids —Fig. 13, and a Bezier patch —Fig. 14. The figures are produced by the algorithm described in [29], while the ridges of Fig. 14 are certified by the algorithm presented in [40]. The color conventions are: blue elliptic (hyperbolic) ridges are painted in blue (green), red elliptic (hyperbolic) ridges are painted in red (yellow). Intersections between ridges are the purple points.

On Fig. 11, the blue principal direction field is drawn —from which one infers that the normal is pointing outward so that the two principal curvatures are negative. The two elliptic ridges are closed curves without turning point. The four Lemon umbilics are the black dots, and they are linked by four separatrices —the yellow and green curves. The separatrices, which are curvature lines, are also ridges in that case. More generally, any line of symmetry is a line of curvature and a ridge ([32, p.162]). Notice also that the lines of curvatures which are not separatrices are all cycles. For each color, they are packed into a cylinder. But this is a non stable configuration since separatrices are umbilical connections, the cycles are not hyperbolic. The medial axis of the ellipsoid is a region homeomorphic to a disk, and is located in the symmetry plane of the two largest axes. This region looks like an ellipsis but is not so [41].

The boundary of the medial axis projects onto the red ridge curve, and reciprocally on this example, every elliptic red ridge point corresponds to a point on the boundary of the medial axis.

Fig.13 is a blend between two ellipsoids defined by the following equation:

$$1-\exp(-0.7(\frac{x^2}{0.15^2}+\frac{y^2}{0.25^2}+\frac{z^2}{0.35^2}-1))-\exp(-0.7(\frac{(x-0.25)^2}{0.1^2}+\frac{(y-0.1)^2}{0.2^2}+\frac{(z-0.1)^2}{0.3^2}-1))=0. \quad (13)$$

This model has six umbilics of index $+1/2$ and two of index $-1/2$. Notice that this complies with the Euler characteristic. One can also observe purple points and turning points.

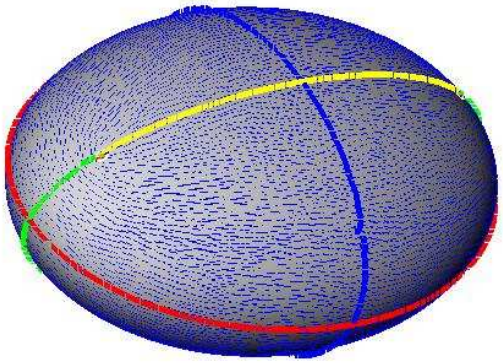

Figure 11: Umbilics, ridges, and principal blue foliation on the ellipsoid

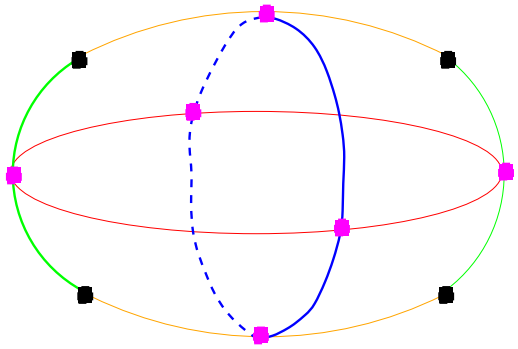

Figure 12: Schematic view of the umbilics and the ridges. Max of k_1: blue; Min of k_1: green; Min of k_2: red; Max of k_2: yellow

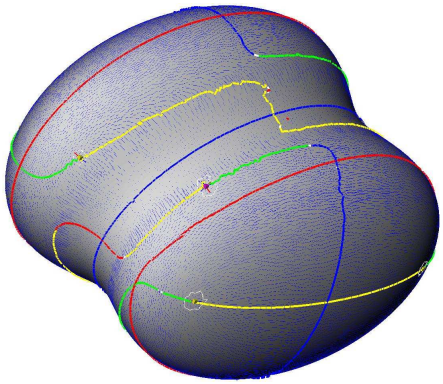

Figure 13: Implicit blending of two ellipsoids (40k points)

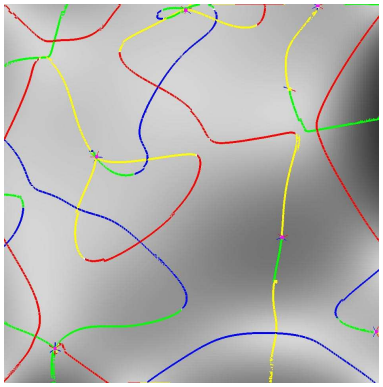

Figure 14: Ridges and umbilics on a Bezier patch

5 Medial axis, skeleton, ridges

5.1 Medial axis of a smooth surface

The medial axis has an outstanding position in many communities and has been rediscovered several times. Example relevant citation are [42, 43] in analysis, [44, 45] in differential geometry, [23, 46, 47, 48] in mathematical morphology. Since we just aim at presenting the local and global structure of the medial axis, we shall follow [20, 49], but the interested reader should also consult [50].

Given a closed manifold S embedded in $\mathbb{R}^3$, the medial axis $MA(S)$ consists of the points of the open set $\mathbb{R}^3\backslash S$ having two or more nearest points on S. A related notion is the skeleton of $\mathbb{R}^3\backslash S$, which consists of the centers of maximal spheres included in $\mathbb{R}^3\backslash S$ —maximal for the inclusion amongst such spheres. For smoothly embedded manifolds, the closure of the medial axis is actually equal to the skeleton, which is why we just refer to the medial axis in the sequel. (Interestingly, applications such as surface

reconstruction, which usually assume the surface to be reconstructed is smooth [17], do not distinguish between medial axis and skeleton.)

Having discussed the contact of a sphere with the surface, let us recall the classification of medial axis points and the corresponding *stratified* structure. While describing ridges, we actually cared more for the surface. For the medial axis, we change the perspective and care for the centers of the maximal spheres. When talking about a contact, one should therefore keep in mind that the corresponding sphere contributes its center to the medial axis.

Since we care for spheres intersecting the surface in an isolated point —otherwise the sphere is not contained in $\mathbb{R}^3\backslash S$, the contact points must correspond to A_1^+ and A_3^+ singularities —refer to Def. 5 for the definition of the A_k^+ types. Notice that an A_1^+ singularity corresponds to a simple tangency. We shall drop the superscript and replace it by the *multiplicity* of the contact, that is A_1^k refers to a sphere having k separate A_1^+ contacts. The medial axis points actually correspond to the following five cases:

- A_1^4, A_1^3, A_1^2 The sphere touches the surface at two, three or four points, and has a simple tangency at each contact point. A_1^4 points are isolated points; A_1^3 points lie on curves, A_1^2 lie on sheets of the medial axis. Moreover, one has the following incidences. At an A_1^4 point, six A_2^1 sheets and four A_1^3 curves meet. Along an A_1^3 curve, three A_1^2 sheets meet.
- A_3^+ The contact point is an elliptic ridge point. The corresponding medial axis points bound A_1^2 sheets.
- $A_3^+A_1$ The sphere has two contact points. The center of the sphere lies at the intersection between an A_1^3 curve together with an A_3^+ curve. This is where an A_1^2 sheet vanishes.

An example consisting of a surface with two sheets is presented on Fig. 15. We describe it through a plane sweep from top to bottom. The top part consists of two sheets swept by two simple curves of roughly triangular and circular section. Then the inner contour vanishes so that we are left with the outer sheet which is roughly speaking a cylinder of triangular section. Then, section of the cylinder changes from triangular to elliptic. Eventually, the cylinder splits into two legs of elliptic sections. Near the top, the structure of the medial axis is that of a tetrahedron, with six A_1^2 sheets and four A_1^3 curves meeting. The boundary of each sheet consists of an A_3 curve. When the section gets rounder, one A_2 sheet vanishes at an A_3A_1 point.

There is an intuitive way to understand the preceding results, by counting separately the numbers of degrees of freedom and the number of constraints attached to a particular medial axis point. To see how, recall that a contact involves one sphere and one or more points on the surface. In terms of degrees of freedom (dof), a sphere yields four degrees of freedom, choosing a point on a surface is another two dof, and choosing a point on a curve drawn on a surface is one dof. In terms of constraints at the contact points, constraining a sphere to have an A_1 contact imposes three constraints. (Indeed the tangent plane being set to that of the surface at p, we are left with the choice of the radius —which defines the pencil of spheres through the contact point.) Similarly, having an A_3 contact imposes four degrees of freedom since the radius of the sphere has to be one of the principal curvatures. Let us now discuss the different cases:

- A_1^2 Having two contacts of order one imposes $2.3 = 6$ constraints. But choosing two points on S together with the contact spheres yields $2.2 + 4 = 8$ dof. One can expect A_1^2 points to lie on sheets.
- A_1^3 Three A_1 contacts define $3.3 = 9$ constraints, and $3.2 + 4 = 10$ dof. A_1^3 points are expected to lie on curves.
- A_1^4 Four A_1 yield $4.3 = 12$ constraints and $4.2 + 4 = 12$ dof. These medial axis points are expected to be isolated.
- A_3 Such a point yields 4 constraints. In terms of dof, and since A_3 points lie on curves on the surface, we have one dof for the choice of the contact point, and four for the sphere. A_3 contacts are therefore expected along curves.
- A_3A_1 The contact points respectively yield $4 + 3$ constraints. On the other hand, choosing one point along a curve, another on the surface, together with the dof of the sphere yield $2 + 1 + 4$ dof. Such contacts are expected to be isolated.

5.2 Medial axis and ridges

Spheres centered on the boundary of the medial axis project onto elliptic ridge points of type A_3^+ on the surface. But an elliptic ridge point can fail to be the contact of a point of the boundary of the MA in two cases: (i) if the limiting bitangent sphere crosses the surface away from the ridge point or (ii) if the surface is locally inside this sphere. (This latter case happens in elliptic regions for a positive minimum of k_2 or a negative maximum of k_1). In the first case, the sphere is not contained in $\mathbb{R}^3 \backslash S$, and in the second it is not maximal for inclusion.

Fig. 16 illustrated case (i), the lowest point is an elliptic ridge point but its bitangent sphere has a non local intersection with the curve. Fig. 11 illustrates case (ii), the blue elliptic ridge is the loci of negative maximum of k_1. The MA, which is an ellipsoid in the equatorial plane (spanned by the two longest principal axis of the ellipsoid), only gives birth to the red ridge (negative minimum of k_2).

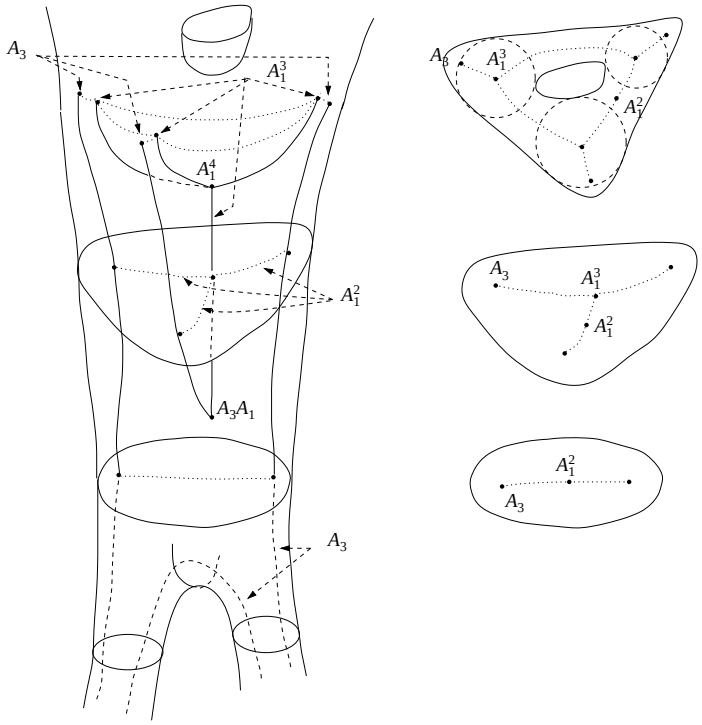

Figure 15: The stratified structure of the medial axis of a smooth surface

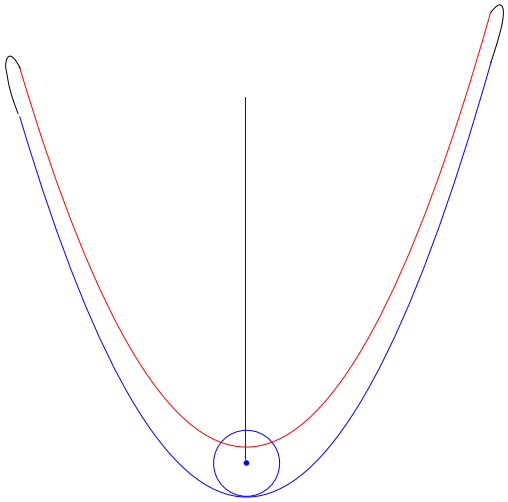

Figure 16: An extrema of curvature not image of the medial axis boundary

6 Topological equivalence between embedded surfaces

Having discussed delicate differential notions in the previous sections, we finish up with a seemingly simpler question: what is the right notion of equivalence for embedded surfaces of E^3, and what are sufficient conditions for two surfaces two be equivalent? Interestingly, the later question can be related to properties of the medial axis. We focus on surfaces embedded in E^3, orientable and without boundary, and which are either smooth —i.e. at least C^2— or piecewise linear.

6.1 Homeomorphy, isotopy, ambient isotopy

A well known Theorem [51, Thm 5.1] states that for surfaces, the genus characterizes the topology:

Theorem. 5 *Two connected compact orientable surfaces without boundary are homeomorphic iff they have the same genus.*

Nevertheless, homeomorphy is not the relevant notion for topological equivalence of embedded surfaces. For example, a torus and a knotted torus are homeomorphic, while the two surfaces are obviously not equivalent as embedded surfaces of E^3. Intuitively, two surfaces are equivalent if one can continuously deform one into the other without introducing self-intersection. The natural notion is that of isotopy since it is an equivalence between embeddings. There are two slightly different notions: isotopy and ambient isotopy.

Definition. 7 *Let S and S' be two surfaces embedded in E^3.*

- *S and S' are isotopic if there is a continuous map $F : S \times [0,1] \to E^3$ such that $F(.,0)$ is the identity of S, $F(S,1) = S'$, and for each $t \in [0,1]$, $F(.,t)$ is a homeomorphism onto its image.*
- *S and S' are ambient isotopic if there is a continuous map $F : E^3 \times [0,1] \to E^3$ such that $F(.,0)$ is the identity of E^3, $F(S,1) = S'$, and for each $t \in [0,1]$, $F(.,t)$ is a homeomorphism of E^3.*

In our study of compact surfaces embedded in E^3, the following theorem [52, p.180] shows the equivalence of these two definitions, so we will merely speak of isotopy.

Theorem. 6 *Let $S \subset M$ be a compact submanifold of M a manifold without boundary and $F : S \times [0,1] \to M$ an isotopy of S, then F extends to a ambient isotopy of M.*

Isotopy between embedded surfaces is a topological characteristic of their embeddings, hence it does not interfer with the geometry. F. Chazal et al. [6] give a purely topological condition for isotopy as well as applications to the concepts of medial axis and local feature size. They define the notion of topological thickening of a surface:

Definition. 8 *A topological thickening of S is a set $M \subset E^3$ such that there exists a homeomorphism $\Phi : S \times [0,1] \to M$ satisfying $\Phi(S \times \{1/2\}) = S \subset M$.*

The boundary of a topological thickening M of S thus is the union of $\Phi(\partial S \times [0,1])$ and two surfaces, $\Phi(S,0)$ and $\Phi(S,1)$, which will be referred to as the sides of M. Another surface S' is said to separate the sides of M if one cannot go from one side to the other without crossing S' or leaving M. We are then able to state their main theorem and two corollaries:

Theorem. 7 *Suppose that S (resp. S') is included in a topological thickening M' of S' (resp. M of S), and that S (resp. S') separates the sides of M' (resp. M). Then S and S' are isotopic.*

6.2 Geometric conditions for isotopy

Although isotopy is a topological property, sufficient conditions for isotopy can be obtained using geometric arguments, and in particular properties of the medial axis.

If S is smooth, for $s \in S$, the local feature size of s is defined as the Euclidean distance to the medial axis, that is $\mathrm{lfs}(s) = d(s, MA(S))$ —see [17]. (As observed in section 5, since the surface is smooth the medial axis is closed, so that the Euclidean distance is a minimum and not an infimum.) Moreover, $\mathrm{lfs}(S)$ is defined as the number $\inf_{s \in S} d(s, MA(S))$. S being at least C_2, one has $\mathrm{lfs}(S) > 0$ cf. [53, 54]. The following is proved in [6]:

Corollary. 1 *Let S and S' be compact orientable smooth surfaces without boundary.*

- *If each connected component of S (resp. S') encloses exactly one connected component of $MA(S')$ (resp. $MA(S)$), then S and S' are isotopic.*
- *If the Hausdorff distance $H(S,S')$ between the two surfaces is such that $H(S,S') < \min(lfs(S), lfs(S'))$, then S and S' are isotopic.*

Roughly speaking, one proves that S and S' are isotopic by first finding a neighborhood of S in E^3 which contains S' and second deforming S' to S most of the time with the normal projection onto S in E^3.

Using the global bound $\mathrm{lfs}(S)$ and ε-neighborhoods, Sakkalis et al. [5] give a family of surfaces which are isotopic to S. Suppose S is smooth and oriented, for $\rho \in \mathbb{R}$, $S_o(\rho) = \{s + \rho n_s | s \in S\}$ is the offset surface of S. They show that for $|\rho| < \mathrm{lfs}(S)$ offset surfaces are smooth surfaces embedded in E^3 and are isotopic to S. Moreover each point of the offset has a unique nearest point on S.

With the same kind of arguments, Amenta et al. [1] show the isotopy between a smooth surface and a piecewise linear approximation. More precisely, Amenta at al. [2] presented an algorithm to extract a piecewise linear surface T from the Delaunay triangulation of a ε-sample of S. The projection from T to its nearest point on S is a homeomorphism which is used to construct the isotopy. The advantage of this method is that the approximating surface needs not to stay in a ε-neighborhood globally defined.

7 Conclusion

We surveyed the notions of umbilics, lines of curvatures, foliations, ridges, medial axis, and topological equivalences for smooth embedded surfaces, with an emphasis on global structure theorems.

An important aspect which has been eluded is the dynamic case, that is the structure theorems valid if one replace a surface by say a one-parameter family of surfaces. Of particular interest in that case are the birth and death phenomena. These indeed feature transitions between patterns observed in the static case, and the time events between them are a measure of persistence of the objects involved. The reader is referred to [25, 26, 55] [16, chap.7] for pointers in that direction concerning ridges and MA. Note that it does not make sense to study a single line of curvature dynamically. One has to consider the topology of the principal foliation instead, this is usually referred as bifurcation theory, see [56].

From a practical perspective, we expect this survey to provide incentives to develop certified surface approximation algorithms.

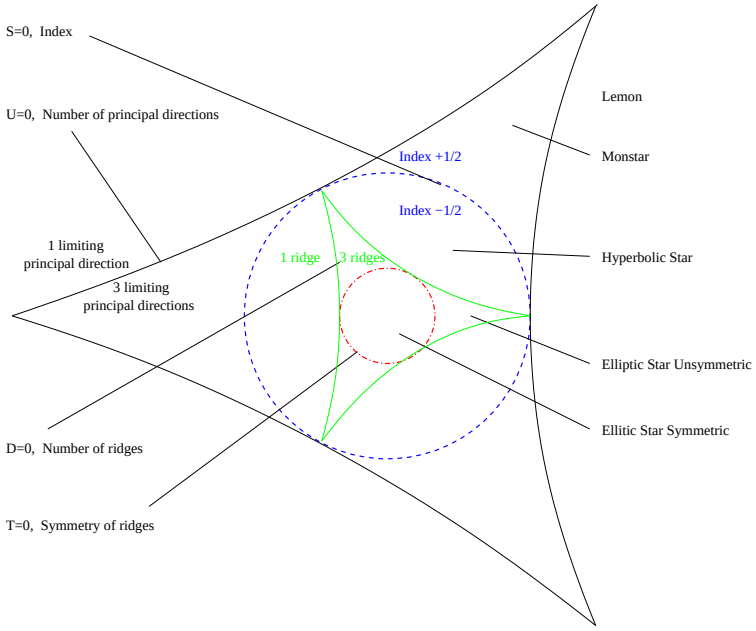

Figure 17: Umbilic classification in the complex plan

Acknowledgements

Abdelkrim Mebarki is acknowledged for producing the plots of Fig. 2 with his software `StreamLines_2` —to be released as a CGAL package.

This research has been partially supported by the *Effective Computational Geometry for Curves and Surfaces* European project, Project No IST-2000-26473.

A Appendix: Umbilic classification in the complex plane

The classification of umbilics with respect to the cubic part of the Monge form of the surface can be illustrated by a diagram in the plane (Fig. 17). With a change of variables which corresponds to a rotation in the tangent plane and noting $\zeta = x + iy$ the cubic form $b_0x^3 + 3b_1x^2y + 3b_2xy^2 + b_3y^3$ becomes $Re(\zeta^3 + \omega\zeta^2\bar{\zeta})$ for some complex number ω. Then umbilics are parameterized by ω in the complex plane. The zero sets of the four invariants S, U, D and T give four curves partitioning the plane in sectors. Umbilics on the complement of these curves are generic.

References

[1] N. Amenta, T. Peters, and A. Russell. Computational topology: ambient isotopic approximation of 2-manifolds. *Theoretical Computer Science*, 305:3–15, 2003.

[2] N. Amenta, S. Choi, T. K. Dey, and N. Leekha. A simple algorithm for homeomorphic surface reconstruction. In *Proc. 16th Annu. ACM Sympos. Comput. Geom.*, pages 213–222, 2000.

[3] J.-D. Boissonnat, D. Cohen-Steiner, and G. Vegter. Meshing an implicit surface with certified topology. In *ACM STOC*, 2004.

[4] J.-D. Boissonnat and S. Oudot. Provably good surface sampling and approximation. In *Symp. on Geometry Processing*, 2003.

[5] T. Sakkalis and T. Peters. Ambient isotopic approximations for surface reconstruction and interval solids. In *ACM Symposium on Solid Modeling*, 2003.

[6] F. Chazal and D. Cohen-Steiner. A condition for isotopic approximation. In *ACM Symposium on Solid Modeling*, 2004.

[7] S. Petitjean. A survey of methods for recovering quadrics in triangle meshes. *ACM Computing Surveys*, 34(2), 2001.

[8] V. Borrelli, F. Cazals, and J-M. Morvan. On the angular defect of triangulations and the pointwise approximation of curvatures. *Comput. Aided Geom. Design*, 20, 2003.

[9] F. Cazals and M. Pouget. Estimating differential quantities using polynomial fitting of osculating jets. *Computer Aided Geometric Design*, 22(2), 2005. Conference version: Symp. on Geometry Processing 2003.

[10] D. Cohen-Steiner and J.-M. Morvan. Restricted delaunay triangulations and normal cycle. In *ACM Symposium on Computational Geometry*, 2003.

[11] J-M. Morvan and B. Thibert. Smooth surface and triangular mesh : Comparison of the area, the normals and the unfolding. In *ACM Symposium on Solid Modeling and Applications*, 2002.

[12] Pierre Alliez, David Cohen-Steiner, Olivier Devillers, Bruno Levy, and Mathieu Desbrun. Anisotropic polygonal remeshing. *ACM Transactions on Graphics*, 2003. SIGGRAPH '2003 Conference Proceedings.

[13] T. Delmarcelle and L. Hesselink. The topology of symmetric, second-order tensor fields. In *IEEE Visualization Proceeedings*, pages 104–145, 1994.

[14] X. Pennec, N. Ayache, and J.-P. Thirion. Landmark-based registration using features identified through differential geometry. In I. Bankman, editor, *Handbook of Medical Imaging*. Academic Press, 2000.

[15] K. Watanabe and A.G. Belyaev. Detection of salient curvature features on polygonal surfaces. In *Eurographics*, 2001.

[16] P. W. Hallinan, G. Gordon, A.L. Yuille, P. Giblin, and D. Mumford. *Two-and Three-Dimensional Patterns of the Face*. A.K.Peters, 1999.

[17] Nina Amenta and Marshall Bern. Surface reconstruction by Voronoi filtering. *Discrete Comput. Geom.*, 22(4):481–504, 1999.

[18] J.-D. Boissonnat and F. Cazals. Natural neighbor coordinates of points on a surface. *Comput. Geom. Theory Appl.*, 19:155–173, 2001.

[19] T. K. Dey and W. Zhao. Approximate medial axis as a voronoi subcomplex. In *ACM Sympos. Solid Modeling and Applications*, 2002.

[20] J. Bruce, P. Giblin, and C. Gibson. Symmetry sets. *Proc. Roy Soc Edinburgh Sect. A*, 101, 1985.

[21] L. Hormander. *Notions of convexity*. Birkhauser, 1994.

[22] F.H. Clarke. *Nonsmooth Analysis and Control Theory*. Springer, 1997.

[23] J. Serra. *Image Analysis and Mathematical Morphology*. Academic Press, London, UK, 1982.

[24] A. Lieutier. Any open bounded subset of $\mathbb{R}^n$ has the same homotopy type than its medial axis. In *ACM Solid Modeling*, 2003.

[25] J. Bruce and P. Giblin. Growth, motion and 1-parameter families of symmetry sets. *Proc. R. Soc. Edinb., Sect. A*, 104, 1986.

[26] P. Giblin and B. Kimia. Transitions of the 3d medial axis under a one-parameter family of deformations. *ECCV*, 1, 2002.

[27] J. Damon. On the smoothness and geometry of boundaries associated to skeletal structures ii: Geometry in the blum case. *Compositio Mathematica*, 140(6), 2004.

[28] F. Chazal and A. Lieutier. The lambda medial axis. *Graphical Models*, To Appear, 2005.

[29] F. Cazals and M. Pouget. Topology driven algorithms for ridge extraction on meshes. Technical Report RR-5526, INRIA, 2005.

[30] C. Gutierez and J Sotomayor. *Lines of Curvature and Umbilical Points on Surfaces*. IMPA, 1991.

[31] R. Morris. *Symmetry of curves and the geometry of surfaces: two explorations with the aid of computer graphics*. PhD thesis, Univ. of Liverpool, 1990.

[32] I. Porteous. *Geometric Differentiation (2nd Edition)*. Cambridge University Press, 2001.

[33] T. Maekawa, F.-E. Wolter, and N. M. Patrikalakis. Umbilics and lines of curvature for shape interrogation. *CAGD*, 13(2):133–161, 1996.

[34] I. Nikolaev. *Foliations on Surfaces*. Springer, 2001.

[35] M. Spivak. *A Comprehensive Introduction to Differential Geometry*, volume 3. Publish or perish, 1999.

[36] I. Porteous. The normal singularities of a submanifold. *J. Diff. Geom.*, 5, 1971.

[37] I. Porteous. Normal singularities of surfaces in $\mathbb{R}^3$. In *Proc. Symp. Pure Math. (40, Part II)*, 1983.

[38] J.W. Bruce and P.J. Giblin. *Curves and singularities (2nd Ed.)*. Cambridge, 1992.

[39] V.I. Arnold. *Catastrophe theory (3rd Ed.)*. Springer, 1992.

[40] F. Cazals, J.-C. Faugeres, M. Pouget, and F. Rouillier. Certified detection of umbilics, parabolic curves, and ridges on polynomial parametric surfaces. *In preparation*, 2005.

[41] W. L. F. Degen. The cut locus of an ellipsoid. *Geometriae Dedicata*, 67(2), 1997.

[42] P. Erdös. On the hausdorff dimension of some sets in euclidean space. *Bull. Am. Math. Soc.*, 52, 1946.

[43] L. Hormander. *The analysis of linear partial differential operators - I*. Springer, 1983.

[44] R. Thom. Sur le cut-locus d'une variete plongee. *J. Differ. Geom.*, 6, 1972.

[45] D. Milman. The central function of the boundary of a domain and its differentiable properties. *J. Geom.*, 14, 1980.

[46] J. Serra, editor. *Image Analysis and Mathematical Morphology, volume 2: Theoretical Advances*. Academic Press, New York, 1988.

[47] Jonathan W. Brandt and V. Ralph Algazi. Computing a stable, connected skeleton from discrete data. In *Proceedings of the 1991 IEEE Computer Society Conference on Computer Vision and Pattern Recognition*, pages 666–667, IEEE Service Center, Piscataway, NJ, USA (IEEE cat n 91CH2983-5), 1991. IEEE.

[48] J. W. Brandt and V. R. Algazi. Continuous skeleton computation by Voronoi diagram. *CVGIP: Image Understanding*, 55(3):329–338, 1992.

[49] P. Giblin and B. Kimia. A formal classification of 3d medial axis points and their local geometry. In *Computer Vision and Pattern Recognition*, Hilton Head, South Carolina, USA, 2000.

[50] Y. Yomdin. On the general structure of a generic central set. *Compositio Math*, 43, 1981.

[51] W. S. Massey. *Algebraic Topology: An Introduction*, volume 56 of *Graduate Texts in Mathematics*. Springer-Verlag, 1977.

[52] M.W. Hirsch. *Differential Topology*. Springer-Verlag, 1988.

[53] H. Federer. Curvature measures. *Trans. Amer. Math. Soc.*, 93:418–491, 1959.

[54] F. E. Wolter. Cut locus and medial axis in global shape interrogation and representation. Technical Report 92-2, MIT, Dept. Ocean Engg., Design Lab, Cambridge, MA 02139, USA, January 1992.

[55] J. Bruce, P. Giblin, and F. Tari. Ridges, crests and sub-parabolic lines of evolving surfaces. *Int. J. Computer Vision*, 18(3):195–210, 1996.

[56] X. Tricoche. *Vector and Tensor Field Topology Simplification, Tracking, and Visualization*. Universitat Kaiserslautern, 2002.